ISSN: 1696-8352

Recent studies on the use of simulated concrete pore solution for corrosion evaluation: a systematic review using prisma

Estudos recentes sobre o uso de solução de poros de concreto simulada para avaliação de corrosão: uma revisão sistemática utilizando prisma

DOI: 10.55905/oelv21n10-040

Recebimento dos originais: 01/09/2023
Aceitação para publicação: 04/10/2023

Maria Carolina de Paula Estevam D'Oliveira
PhD in Biotechnology by Programa de Pós-Graduação em Biodiversidade e Biotecnologia (PPG - BIONORTE)
Institution: Universidade Federal do Tocantins
Address: Avenida ns 15, Quadra 109, Alcno 14, Norte, s/n, bloco D, Plano Diretor Norte, Palmas - TO, CEP: 77001-090
E-mail: carolina.doliveira@uft.edu.br

Salmo Moreira Sidel
PhD in Materials Science
Institution: Universidade Federal do Tocantins
Address: Avenida ns 15, Quadra 109, Alcno 14, Norte, s/n, bloco D, Plano Diretor Norte, Palmas - TO, CEP: 77001-090
E-mail: sidel@uft.edu.br

Patrícia Martins Guarda
PhD in Biotechnology
Institution: Universidade Federal do Tocantins
Address: Avenida ns 15, Quadra 109, Alcno 14, Norte, s/n, bloco D, Plano Diretor Norte, Palmas - TO, CEP: 77001-090
E-mail: patriciaguarda@uft.edu.br

Emerson Adriano Guarda
Doctor in Organic Chemistry
Instituion: Universidade Federal do Tocantins
Adrres: Avenida NS-15, Quadra 109, Alcno 14, Norte, s/n, bloco D, Plano Diretor Norte, Palmas - TO, CEP: 77001-090
Email: emersonprof@uft.edu.br

ABSTRACT

The use of simulated concrete pore solutions (SCP) is a viable alternative for studying the behavior of the steel/concrete interface, mainly due to the possibility of reproducibility in

ISSN: 1696-8352

the laboratory. However, this solution needs to represent the reality of what happens in the concrete pores, regarding the ions present in the solution and a stable pH, close to 12.5. Therefore, this article presents a systematic review of the use of SCP in the assessment of adherence since 2018. The investigation followed the PRISMA protocol. After including/excluding steps, 58 studies were included in the review. After the evaluation of these studies, the results were presented focusing on the types of SCP, the experiments carried out and the resistance monitoring methods that used electrochemical experiments, spectroscopy and image analysis. In short, this methodology makes it possible to identify the main knowledge gaps in this area.

Keywords: simulated concrete pore solution, corrosion, monitoring, electrochemistry, systematic review, prisma.

RESUMO

O uso de soluções de poros de concreto simulado (SPC) é uma alternativa viável para estudo do comportamento da interface aço/concreto, principalmente pela possibilidade de reprodutibilidade dentro do laboratório. No entanto, essa solução precisa representar a realidade do que acontece nos poros do concreto, no que tange aos íons presentes na solução e pH estável, próximo dos 12,5. Portanto, este artigo apresenta uma revisão sistemática quanto ao uso de SPC na avaliação da corrosão desde 2018. A investigação seguiu o protocolo PRISMA. Depois de incluir/excluir etapas, 58 estudos foram incluídos na revisão. Após avalição desses estudos, os resultados foram apresentados focando os tipos de SPC, os experimentos realizados e os métodos de monitoramento da corrosão que utilizaram experimentos eletroquímicos, espectroscopias e análises de imagens. Em suma, essa metodologia possibilita a identificação das principais lacunas de conhecimento nessa área.

Palavras-chave: solução de poros de concreto simulado, corrosão, monitoramento, eletroquímica, revisão sistemática, prisma.

1 INTRODUCTION

Concrete is the most used building material in the world and the second most consumed by mankind, behind only water (HELENE; ANDRADE, 2007), being the most man-made (GU; BEAUDOIN; RAMACHANDRAN, 2001). Its production will reach 10,000 million tons/year, and in the next 30 years it will increase by around 100% (PACHECO-TORGAL et al., 2015).

Reinforced concrete structures are found in the most diverse environments subject to aggressive agents, such as sea salt spray, deicing salts, carbon dioxide present in industrialized areas and many others that can impair performance and decrease durability.

ISSN: 1696-8352

Even being constituted by elements composed of concrete and steel, so that they can act together in the load bearing process of a building, there are many problems that can affect this structure, characterized as simple or complex pathologies, compromising the integrity of the building (RIBEIRO et al., 2013).

In reinforced concrete, there is a phenomenon of steel degradation, which is one of the challenges of civil engineering, the corrosion process. Corrosion is a natural electrochemical phenomenon with progressive detrimental effects on the integrity of materials as well as huge economic losses for various industries (HOU; LI; CHEN, 2018; TRAN et al., 2020).

It is estimated that about 15% to 35% of the overall corrosion cost can be saved by using available corrosion protection strategies. These statistics reveal the important role of corrosion protection methods to improve the life of metal structures and reduce maintenance and repair costs in industries (KOCH, 2017).

Corrosion occurs due to the effectiveness of some agents through degrading mechanisms, as follows: carbonation - transformation of calcium hydroxide into calcium carbonate, which is more neutral, inducing a reduction in the pH of the concrete; depassivation of the reinforcement - happens when the chloride ion breaks the passivation layer, an insoluble layer that protects steel (VITÓRIO, 2003).

Of the cases identified in Brazil, a recent example of damage caused by steel corrosion in structures was the Maracanã stadium in Rio de Janeiro, which underwent a series of investigations and reports for renovation and adaptation to receive the 2014 World Cup. The steel corrosion was the most present and intense pathological manifestation, occurring loss of more than 60% of the steel section, and the consequences of this process as the appearance of cracks and concrete spalling were also observed, especially in the marquee of the stadium in which the report presented by engineers concluded by recommending the demolition of the same, because the structure was too compromised by the corrosive process representing a risk to the safety of users (SOUZA; TAVARES; TEIXEIRA, 2014).

The cost of an intervention for structural recovery goes far beyond the cost of repair services, as it also involves the interdiction of the site, when necessary, transfer of

ISSN: 1696-8352

activities to another location, in addition to the risk that a damaged structure offers to people, materials and equipment (BOLINA; TUTIKIAN; HELENE, 2019).

There are various techniques to protect steel from corrosion attack, such as material modification, alteration in the surrounding environment, surface coating, cathodic protection, and the use of corrosion inhibitors. Some methods rely on moisture/oxygen removal, while others make use of a permanent coating on the metal surface. However, some approaches are based on the conversion of anodic material into a cathode. However, the applications of existing techniques are limited by various constraints. For example, material modification is often impossible or expensive (GENTIL, 1996).

Process environment substitution is not an optional solution in many industrial applications, because the metal has to experience a certain reactive medium. The implementation of some methods, for example, coating, can raise CO2 emissions beyond acceptable levels. In addition, other methods such as cathodic protection require expensive equipment, thus increasing the overall cost. Corrosion inhibitors, however, offer an economical and viable alternative solution (RANI; BASU, 2012).

The purpose of this article is to discuss papers following a systematic review, using the PRISMA protocol, to follow recent progress in the use of simulated concrete pore solution (SCP) for corrosion assessment. The evaluation of the simulated concrete pore solutions, the experiments performed, and the corrosion monitoring methods used in each study are detailed in the following sections.

2 MATERIALS AND METHODS

A Systematic Literature Review seeks to establish a formal survey of the state of the art in a consistent and planned way, aiming to implement criteria for selection of research that may be useful and bring relevant information on the subject under study, being a strategy to reduce predispositions and random errors that can occur in a traditional review (URRA MEDINA; BARRÍA PAILAQUILÉN, 2010). In addition, it consists of the identification and description of previous research, systematic evaluation of research following rigorous protocols, and synthetic and coherent collection of evidence in the

ISSN: 1696-8352

selected research universe (O'CONNOR; SARGEANT; WOOD, 2017). Facilitating tools for carrying out a systematic literature review are used, such as the PRISMA protocol (Preferred Reporting Items for Systematic Reviews and Meta Analyses), which has 17 guidelines composing an information flowchart (MOHER et al., 2015).

Unlike a literature review, which is based on a summary or overview of a particular topic, a systematic literature review is focused on answering a question, eliminating the biases and prejudices. Furthermore, it is important to note that the planning that takes place prior to the review allows others to compare, replicate, and judge the validity of the protocol and review, thus preventing arbitrary decisions regarding the inclusion and exclusion of data (MOHER et al., 2015; O'CONNOR; SARGEANT; WOOD, 2017).

In the area of corrosion assessment using simulated concrete pores (SCP), there is no systematic literature review that follows or adapts the PRISMA methodology, the only systematic review found is related to the use of cement-based materials modified with double hydroxides in layers (LDHs) (ZHAI et al., 2022).

In this context, the objective of this systematic review is to compile data between 2018 and 2022, on the use of simulated concrete pore solutions in corrosion evaluation, using the methodological guidelines defined by the PRISMA protocol (MOHER et al., 2015), and the, Mendeley© software, used to organize the results according to each of the databases, and which also helped in the organization of the data, facilitating the laborious and repetitive process of a systematic literature review.

The articles were selected through the Capes Journals platform (www.periodicos.Capes.gov.br), using CAFE, where it was possible to search the PubMed, Science Direct, Springer and Web of Science databases. The search terms were: ("Concrete pore Solution" AND corrosion). The results were limited to articles in English published between 2018-2022. The identified articles had their titles and abstracts evaluated independently by two reviewers.

Review articles, books and book chapters, conference abstracts and case studies were excluded.

For the next step, the Qualis CAPES concept was used, which is a Brazilian scientific production classification system, based on articles published in journals of all postgraduate programs in the country, where the main objective is to evaluate the quality of scientific production and help teachers and students in the article submission process, and this quality is classified, in descending order, in articles ranging from A1, A2, A3, A4, B1, B2, B3, B4 to C.

The following exclusion criteria were applied: articles with Qualis lower than A2, articles that did not mention, in the title, pores of simulated concrete and corrosion or passivation, articles without full text. Articles were included, compared and duplicate records were removed, reaching a final number of 58 articles of interest.

It is important to point out that this research will relate the articles that evaluated the types of simulated concrete pore solutions, the experiments carried out and the corrosion monitoring methods used.

3 RESULTS AND DISCUSSIONS

The selection of studies is presented in a flowchart according to the requirements of PRISMA (see Figure1), illustrating the number of articles identified, included and excluded, evidencing the reason. The search in PubMed, Science Direct, Springer, and Web of Science databases identified a total of 805 articles. Of these, articles whose year of publication is less than 2018 (468), review articles (4), conference abstracts and case studies (2), those whose Qualis is less than A2 (58), those without full text available (4), excluded for duplication (99), and those that do not mention, in the title, concrete pores and corrosion or passivation (34) were excluded, reaching 136 articles.

Also excluded after reviewing the title, keywords, and abstract (59) were those from other research areas (14). After this step, 63 articles remained of which 5 were excluded after a full text review. Thus, 58 articles were submitted to full text analysis and included in this research (Table 1)

Figure 1. Systematic review flowchart according to PRISMA protocol.

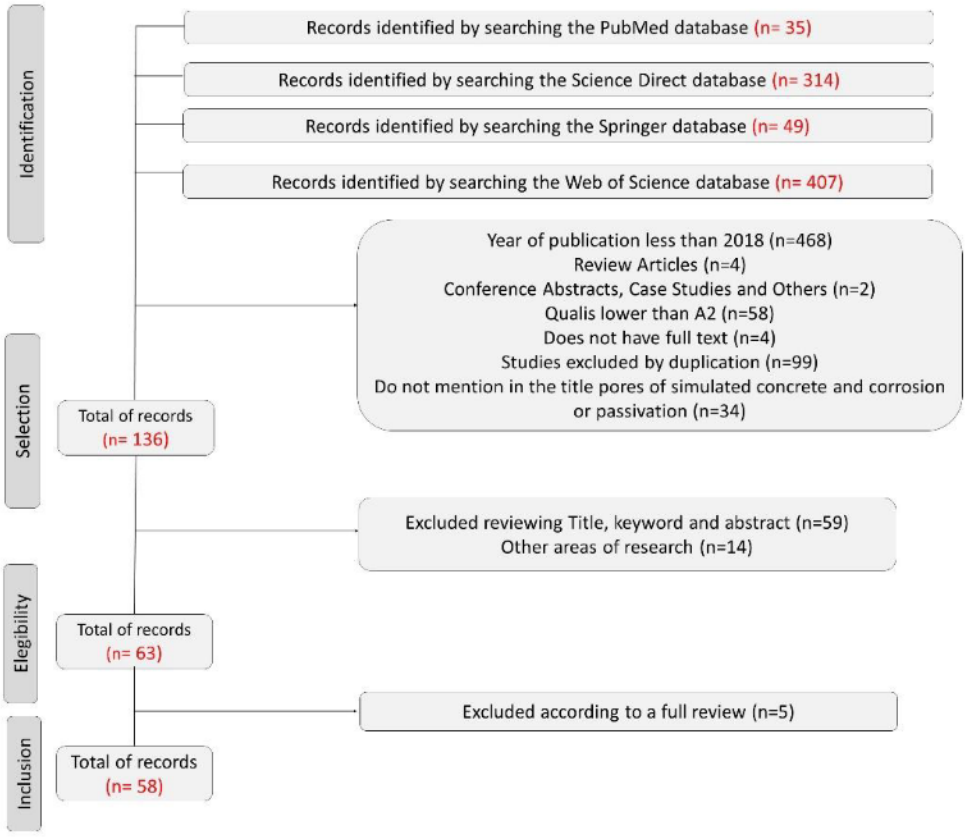

Source: Authors' private collection (May 2023)

Table 1. Summary of systematic literature review: main articles that presented studies on reinforcement corrosion in simulated concrete pore solution

ID	Reference	Simulated pore solutions	Measures
1	(CAO et al., 2019)	Ca(OH)2	XRD; FT-IR; SEM
2	(TEYMOURI et al., 2021)	Ca(OH)2, KOH, NaOH	EIS; MS; XPS.
3	(MANDAL et al., 2020)	CaO, NaOH, KOH	CPP; OCP; EIS; SEM; RAMAN
4	(WU & SHI, 2021)	Ca(OH)2	CV; EIS; CPP; SEM-EDS; AFM; MO; MS
5	(QU et al., 2021)	Ca(OH)2, KOH, NaOH	SEM-EDS; FT-IR; XRD; EIS; LSV
6	(CAI et al., 2021)	Ca(OH)2	OCP; EIS; LPR; XPS; MS
7	(SUBBIAH et al., 2021)	Ca(OH)2, KOH, NaOH	EIS; CPP; FT-IR; DRX; SEM-EDS; AFM; XPS
8	(SHEN & ZHANG, 2022)	Ca(OH)2	XPS; FT-IR; SEM; CPP; EIS
9	(P. XU et al., 2021)	Ca(OH)2	EIS; LSV; SEM; AFM; XPS
10	(ZHAO et al., 2019)	Ca(OH)2, KOH, NaOH	OCP; LPR; EIS; MS; XRD; XPS
11	(LEE et al., 2018)	CaO, NaOH, KOH	OCP; LSV; EIS
12	(W. LIU et al., 2021)	Not Informed	SEM; UV-VIS; XRD; FT-IR; OCP; EIS; CPP

ISSN: 1696-8352

ID	Reference	Simulated pore solutions	Measures
13	(J. XU, TAN, et al., 2020)	Ca(OH)2, KOH, NaOH	Ecorr; EIS; DRX; FT-IR
14	(Y LIU & SHI, 2022)	Ca(OH)2, KOH, NaOH	OCP; EIS; MS; CPP; XPS; AFM; SEM
15	(FENG et al., 2020)	NaOH	OCP; CPP; EIS; XPS; SIMS
16	(YONGQI LIU et al., 2019)	Ca(OH)2	LSV; LPR; EIS; FT-IR; XPS
17	(J. XU, WEI, et al., 2020)	Cement and water	OCP; EIS; SEM; XRD; FT-IR; OM; XPS
18	(ETIM et al., 2021)	Not Informed	SEM-EDS; LSV; XRD; XPS; OCP; EIS
19	(MANSOUR et al., 2018)	Ca(OH)2	LSV; OM; EIS; CV
20	(PENG et al., 2018)	Ca(OH)2, NaOH	OCP; LSV; EIS; MS; XPS; SEM
21	(C. CHEN et al., 2019)	Ca(OH)2	LPR; EIS; XPS
22	(D. WANG et al., 2020)	Cement and water	Ecorr; LPR; EIS; CPP; MS; XPS; SEM
23	(WU et al., 2020)	Ca(OH)2	EIS; LSV; XPS; OM; SEM-EDS; CV
24	(MA et al., 2022)	Ca(OH)2	EIS; OCP; CPP; PZC; SEM; FT-IR; DRX
25	(TIWARI et al., 2021)	Ca(OH)2, KOH, NaOH	CPP; SEM; EDX; XRD; FTIR; UV-Vis
26	(NADERI et al., 2022)	Ca(OH)2, KOH, NaOH	EIS; OCP; XPS; SEM-EDS; FT-IR
27	(GROMBONI et al., 2021)	Cement and water	OCP; EIS; SEM-EDS; XPS
28	(J SHI et al., 2020)	Ca(OH)2, KOH, NaOH	EIS; CV; CPP; AFM; XPS; EPMA; EDS
29	(ZHENG et al., 2021)	Ca(OH)2	FT-IR; OCP; LPR; EIS; CPP; SEM; EDS
30	(ZHENG, DAI, POON, et al., 2018)	Ca(OH)2	OCP; SEM-EDS; XRD; EIS; CV
31	(ZHENG, DAI, LI, et al., 2018)	Ca(OH)2	LPR; EIS; MS; XRD; SEM-EDS.
32	(P. XU et al., 2019)	Ca(OH)2	EIS; CV; MS
33	(ZHI et al., 2020)	Ca(OH)2	LPR; EIS; CPP; XPS
34	(YISHAN WANG et al., 2018)	Ca(OH)2	LSV; PZC; SEM-EDS; XPS; M-IR
35	(LIN & ZUO, 2019)	KOH, NaOH	CPP; EIS; XPS
36	(YAN QI WANG et al., 2018)	Ca(OH)2, KOH	SEM; XPS; XRD; LPR
37	(ZHU & ZHANG, 2021)	Ca(OH)2	OCP; FT-IR; CPP; EIS
38	(VERBRUGGEN et al., 2019)	Ca(OH)2, KOH, NaOH	GDEOS; XPS; RAMAN; SEM; LSV
39	(YUAN et al., 2020)	Ca(OH)2	EIS; XPS; LPR; MO; SEM-EDS
40	(M. CHEN et al., 2021)	Ca(OH)2	OCP; LPR; EIS; SEM
41	(JIN et al., 2022)	Ca(OH)2, KOH, NaOH	EIS; XPS; AFM
42	(J SHI et al., 2018)	Ca(OH)2, KOH, NaOH	EIS; OCP; CPP
43	(TEYMOURI et al., 2022)	Ca(OH)2, KOH	OCP; CPP; EIS; MS; SEM; EDS; XPS
44	(YANG et al., 2019)	Ca(OH)2, KOH, NaOH	OCP; EIS; SEM-EDS; FT-IR
45	(ZUO et al., 2019)	Ca(OH)2	FT-IR; SEM; TG-DSC; EIS; LPR

ID	Reference	Simulated pore solutions	Measures
46	(XIONG et al., 2018)	Ca(OH)2, KOH, NaOH	OCP; LPR; EIS; SEM-EDS;
47	(YE WANG et al., 2021)	Ca(OH)2	EIS; OCP; SEM; DRX; FIB; EDS
48	(SINGH et al., 2021)	CaO, NaOH, KOH	CPP; OCP; EIS; SEM; XPS; RAMAN
49	(JINJIE SHI et al., 2021)	Cement and water	OCP; EIS; MS; XPS; SEM-EDS; AFM
50	(ZHANG et al., 2019)	Ca(OH)2, KOH, NaOH	EIS
51	(YAO et al., 2022)	Cement and water.	EIS; CV; CPP
52	(JOHARI et al., 2021)	Ca(OH)2, KOH, NaOH	EIS; LSV; OCP; SEM; AFM; XPS
53	(FAZAYEL et al., 2018)	Ca(OH)2	FT-IR; LPR; EIS; SEM-EDS; AFM
54	(TIAN et al., 2020)	Ca(OH)2	EIS; OM; OCP; XPS; MS
55	(HU et al., 2021)	Ca(OH)2, NaOH	EIS; CPP; OCP; SEM; EDS; RAMAN
56	(NADERI et al., 2021)	Ca(OH)2, KOH, NaOH	XPS; SEM-EDS
57	(SONG, ZHANG, et al., 2021)	Ca(OH)2	OCP; EIS; XPS
58	(SONG, LIU, et al., 2021)	NaNO2-E51/UF encapsulated	LSV; EIS

Source: Authors organization

Studies on the corrosion of reinforced concrete using steel work electrodes of civil construction immersed in concrete pore solutions were initiated in the whose purpose was to solve the problem of the uncertainty of electrochemical measurements and the high resistivity of reinforced concrete. The idea was to extract pore solutions from concrete by means of a pressurizing device in order to characterize them. The technique, however, depended on sophisticated equipment and the amount of solution extracted from each sample was very small (LONGUET, 1973).

For this reason, in 1996 it was proposed the simulation of concrete pore solution by preparing pH solutions similar to those of concrete pores made of saturated Ca(OH)2 or simulated concrete solution made of NaOH, KOH and Ca(OH)2, since these compounds are the most abundant in the pore solution of concrete. Thus, steel samples were prepared and immersed in these alkaline solutions, facilitating the execution of electrochemical measures (L.T. MAMMOLITI; BROWN; HOPE, 1996). From this study, several researchers used the preparation of SCP to study the corrosion of steel, mainly from the decade of 2010.

As already informed in this paper, a temporal cut was made between 2018 and mid-2022. The number of articles was higher in 2021 (Figure 2). In the year 2022, until

August, when the data were compiled, there were already 7 works in this area, and more studies are expected. The systematic review allowed to track which types of pore solutions of simulated concrete were studied, the types of experiments used, the method of corrosion monitoring evaluated.

The liquid phase of the concrete, called pore solution, has an alkaline pH with typical values between 12.5 and 13.5, because of the main constituents of the solution that are alkaline. Its composition is basically composed of sodium hydroxide (NaOH), potassium hydroxide (KOH) and saturated calcium hydroxide (Ca(OH)2) (POURSAEE; ANGST, 2023). Although Ca (OH)2 is also alkaline, the pH above 13 is maintained, mostly, by hydroxyls from NaOH and KOH (POURSAEE, 2010). In this pH range, it is feasible to use steel reinforcement together with concrete, considering that at these hydrogenic potentials the reinforcement remains in a passivation state (METHA; MONTEIRO, 2014).

Figure 2. Published studies found in this systematic review on simulated concrete pores per year since 2018.

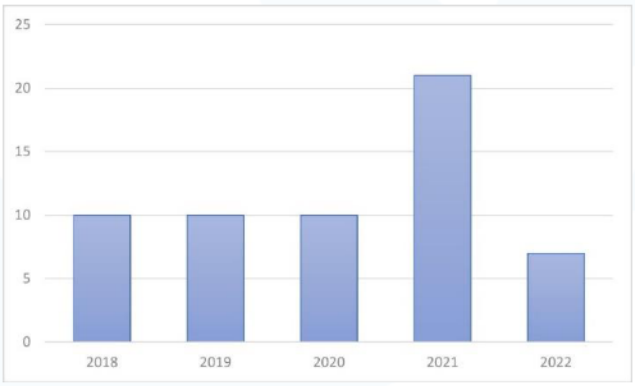

Source: Authors' private collection (May 2023)

Some studies, which took into account the liquid phase of concrete, demonstrate that these solutions are mostly composed of K+ and Na+ ions, representing up to 95% of the alkalis present in the liquid phase of concretes, the other 5% were Ca2+, Mg2+ and S4+ (KEMPL; ÇOPUROGLU, 2015). Regarding Ca2+ ions, its lower concentration is expected due to its low solubility in the usual pH range of concrete (SCOTT; ALEXANDRE, 2016). The composition of the liquid phase also changes with the

ISSN: 1696-8352

presence of external agents such as chlorides and CO2. It was also found that after carbonation there was a decrease in the concentration of Na+ and K+ from approximately 95% to 5.1%. On the other hand, there was an increase in concentrations of S4+ (53.6%), Ca2+ (28.2%) and Mg2+ (13.1%) (KEMPL; ÇOPUROGLU, 2015).

Some authors show that the characteristics of cement, the presence of additions and substitutions by supplementary cementitious materials, the water/cement ratio, the degree of hydration and the external environment influence the composition of the pore liquid phase (KULAKOWSKI, 2002; SCOTT; ALEXANDRE, 2016). In this sense, studies were performed by extracting the solution from the pores to determine the influence of the solution on the durability of the concrete (ORTOLAN, 2015; PLUSQUELLEC et al., 2017; SCOTT; ALEXANDRE, 2016).

Corrosion occurs due to the effectiveness of some agents through degrading mechanisms such as carbonation and depassivation of the steel reinforcement. Figure 3 shows the carbonation front and the change in concrete pH over time. Carbonation starts from the concrete surface and a carbonation front is formed. Then two different pH zones are formed, one with pH still in the natural state of the concrete, around 12 to 13, and another with pH close to 8 (BAKKER, 1988; METHA; MONTEIRO, 2014).

With the ingress of CO2 through concrete in time and the reactions of this gas with calcium hydroxide (Ca(OH)2) available in the cementing matrix occurs the formation of calcium carbonate (CaCO3), and the consequent reduction of the pH of the concrete. When this process reaches the vicinity of the steel reinforcement, it is said that it is depassivated, being susceptible to corrosion. With this, the carbonation front imposes itself inside the concrete and can reach the reinforcement, causing depassivation of the steel, which happens when the chloride ion breaks the passivation layer, which is the layer that protects the steel.

ISSN: 1696-8352

Figure 3. Representation based on the advance of carbonation and pH change in concrete over time

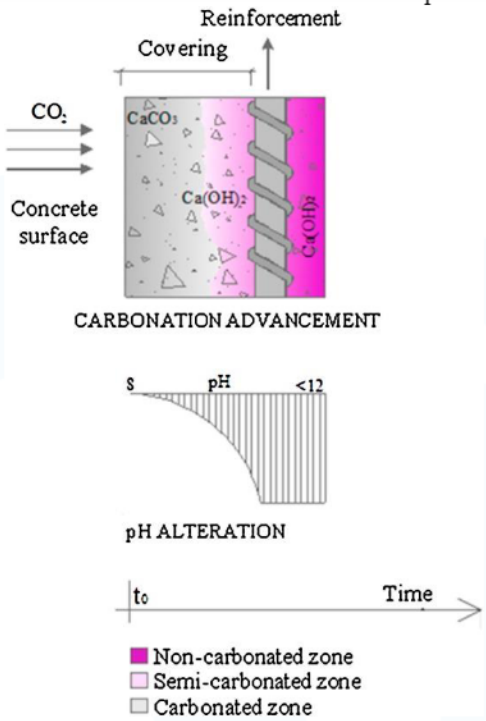

Source: (POSSAN et al., 2017)

Another form of study is through the reproduction of solutions in the laboratory (XU et al., 2019). The use of synthetic solutions for evaluation of chemical processes of cementitious composites is used to facilitate electrochemical analysis, allowing more precise investigations on the influence of chemical compositions, allows a greater control of the variables under study, in addition to reducing the testing time (LIU et al., 2017). Given the above, the articles were classified based on the simulated concrete pore solution (SCP), (Figure 4), electrochemical experiments (Figure 5), spectroscopy (Figure 9) and image analysis (Figure 15).

For the most part, the authors simply adopt a type of SCP composition, not to mention the reason for choosing the chemical composition. Some researchers, however, conducted preliminary study to choose the best SCP composition for the analyses.

As can be seen in Figure 4, there are several ways of producing solution to simulate the environment found in the concrete pores that researchers use to compose the SCP. Although over the years authors have chosen to use a more complex solution, most use saturated Ca(OH)2 solution to simulate the concrete pores (BEN MANSOUR;

DHOUIBI; IDRISSI, 2018; CHEN et al., 2021; TEYMOURI et al., 2022; XU et al., 2019; ZHI et al., 2020).

Figure 4. Types of simulated concrete pore solution used in studies since 2018.

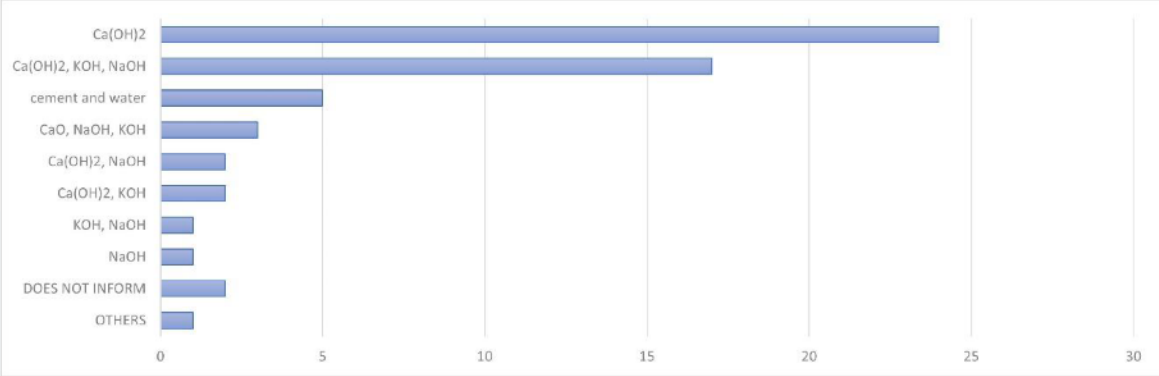

Source: Authors' private collection (May 2023)

Some authors chose to reproduce the alkaline environment of concrete using the mixture of cement and water (GROMBONI et al., 2021; SHI et al., 2020, 2021; XU; TAN; MEI, 2020; YAO et al., 2022). Approaching the reality of concrete production, it was suggested to elaborate a simulated concrete pore solution by mixing all the components of concrete (water, coarse and fine aggregate and cement) with a larger amount of water so that cement hydration was not enough to solidify the mixture(KAPAT; PRADHAN; BHATTACHARJEE, 2006). On the other hand, there were those who chose to extract the powder from cured concrete specimens by mixing it in water to extract the soluble compounds and produce the simulated pore solution (PRADHAN; BHATTACHARJEE, 2007; SHAHEEN; PRADHAN, 2017). It is believed, therefore, that these works are closer to the work reality, because they use the concrete components to produce the SCP. Although aggregates are considered potentially inert in some cases, it is known that there is no guarantee that there is no soluble portion of these materials in water.

In addition, the researchers evaluated the difference between the passive film grown naturally in alkaline solutions and the film grown by anodic polarization. (VELEVA et al., 2002).

ISSN: 1696-8352

Jiang et al (2012) evaluated the influence of the type of salt (KCl, NaCl, CaCl2 and MgCl2) on the threshold value for corrosion initiation of steels in SCP. The solutions used were: 1) saturated solution of Ca (OH)2; 2) cement solution obtained from 20 g of Portland cement dissolved in 2 liters of distilled water. Samples of the steel used in the research were immersed for seven days in each of the solutions, to ensure that they were passivated before being attacked by chlorides. The pH of the solutions was measured after the addition of the salts, being possible to observe that there is no great difference in the behavior of the pH variation with addition of each of the chlorides in solutions 1 and 2. However, as solution 2, due to Portland cement hydration, contains a series of ions (Na+ K+, Ca2+, Mg2+, Al3+ and (SO4)2-), the chlorine ions are physically adsorbed by the CSH (hydrated calcium silicate) and C3A (tri-calcium aluminate) chemically binds the chlorides to produce Friedel's salt (C3A.CaCl2.10H2O), which ensures that the steel has a lower risk of corrosion, as it promotes the removal of a portion of the chlorine ions from the solution. In the saturated solution of Ca(OH)2, the only corrosion inhibitor is the concentration of hydroxyl, which determines the limit of chlorides to initiate corrosion of steel (JIANG et al., 2012). Thus, the authors conclude that the cement solution is more representative of reality.

Although the studies for evaluation of corrosion in reinforced concrete have been carried out through several techniques, the ones that stand out are the electrochemical ones. These techniques, in addition to analysing corrosion as an electrochemical phenomenon and therefore more reliable, have the advantage of being fast and not causing serious damage, such as the destruction of the analyzed specimen at the time of its application; and can be used both in the laboratory and in the field.

Figure 5 illustrates the main electrochemical techniques used for corrosion evaluation of steel immersed in simulated concrete pore solutions. The most used technique is the monitoring of the open potential circuit (OPC), followed by the techniques for obtaining curves and polarization resistance (Rp), which are: cyclic potentiodynamic polarization (CPP), linear polarization resistance (LPR) and scanning linear voltammetry (SLV).

ISSN: 1696-8352

Figure 5. Electrochemical experiments used in the evaluation of simulated concrete pore solutions used in studies since 2018.

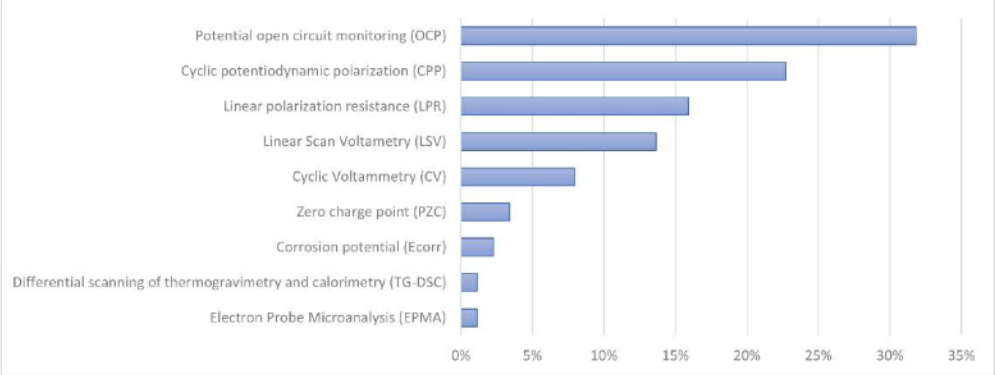

Source: Authors' private collection (May 2023)

Open potential circuit (OPC) monitoring is an electrochemical technique used to initiate most material analyses, especially when it is intended to evaluate the formation of passivating oxide films or corrosive oxides on a metal. It is one of the simplest and most fundamental methods of electrochemistry and the most used in civil engineering to evaluate the corrosion potential by C876-15 (ASTM, 2015). The technique consists of measuring the potential difference between a reference electrode (RE) and the working electrode (WE), immersed in an electrolyte of interest, over time. For this, you can use a simple device, such as a multimeter or a more elaborate one, such as a potentiostat/galvanostat. When a metal is immersed in an electrolyte solution, an electrochemical potential difference (electrical and chemical in nature) occurs between the two phases, the liquid and the solid.

While the electrical double layer (EDL) is formed by organizing ions on the metal surface to stabilize the potential at the metal-solution interface, chemical reactions at the surface cause oscillations in the potential at the metal-solution interface. The formation of the double layer is fast, but the formation of passivating films can have slow growth kinetics (ZIMER, 2009). Thus, with OPC one can track the film growth during potential stabilization.

With the OPC measurement, it is possible to draw a graph similar to the graph in Figure 6 (PENG et al., 2018), which presents the open circuit potential measurements in volts versus a reference electrode (ordered axis) in each time unit (abscissa axis). Before

the complete formation of EDL, the system is not yet in balance. In the case of oxidation of metals in OPC, there is first more oxidation than reduction. Thus, OPC varies constantly until the dynamic equilibrium state is reached. In this state, the chemical reactions are balanced and the OPC ceases to vary, becoming constant. This experiment provides thermodynamic information about the system and serves as an indicator of corrosion or steel passivation (ZIMER, 2009).

Figure 6. Open circuit potential monitoring graph model.

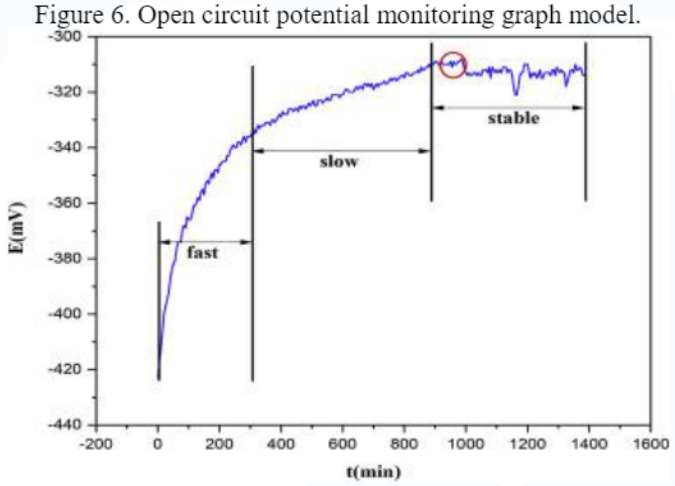

Source: (PENG et al., 2018)

It is worth mentioning again that the level of potential stabilization indicates the moment of high probability that the formation of a passivating film on the surface of the metal has started. In this way, it is possible to find out how long it takes for the formation of a passivation film to be studied.

Most authors perform this measurement based on C876-15 (ASTM, 2015), because they intend to evaluate reinforcement corrosion in aggressive environment (OGUNSANYA; HANSSON, 2019; YANG et al., 2019; ZHAO, Yazhou et al., 2019). Thus, these authors use the reference electrode recommended by the standard, the saturated calomel electrode (SCE). When the researcher's objective is to evaluate the formation of the passivating film, automatic monitoring over a short time interval (maximum one hour) is recommended to observe the change in the electrochemical behavior of the system. Furthermore, SCE should not be used for film formation

ISSN: 1696-8352

measurements because this electrode is not stable in a highly alkaline medium, as is the case with SCP [46]. It is recommended to use an Hg/HgO or Ag/AgCl.

Steel rebars exposed to SCP solution with 3% inhibitor + 3.5% by weight of NaCl contain a significant amount of H+ ions and phosphate ions. H+ and Cl- ions induce corrosion reaction while phosphate ions transform unstable corrosion products into a stable iron phosphate as passive film, respectively. Thus, it is seen that as the exposure periods are increased, the OPC is shifted to a more noble/positive direction. The steel reinforcement, without a passivating layer, has initially deteriorated due to Cl- ions and forms the corrosion products, thus active OPC is observed by 1 h of exposure. However, when the exposure period reaches 24 h to 120 h, these corrosion products deposit on the rebar surface, shifting the OPC to a positive, nobler direction (MANDAL et al., 2020).

The OPC evolution of Q235 carbon steel in SPC with 0.25 mols/L of NaCl and different concentrations of triethanolammonium dodecylbenzene sulfonate (TDS) was evaluated for 8 hours. In the initial 4 h, the OPC of all carbon steel samples immersed in the porous solution presents a declining trend, probably due to the corrosive effect of chloride and carbonation ions; after that, a relatively stable potential value was observed. After 8 h of immersion, the OPC of the sample in the solution without TDS decreased slowly. However, for the solution with TDS, it increases marginally. This can be explained by the adsorption of TDS molecules in carbon steel Q235, which prevent chloride ions from coming into contact with the surface of the steel and repassing the metastable pitting. At the end of immersion, the OPC of the samples in the solution with TDS are much higher than in the solution without TDS and the higher the concentration, the greater the potential (ZHAO, Y et al., 2019).

The great deficiency of this technique is that its values indicate the balance between the anodic and cathodic reaction, without offering quantitative information, that is, it is not possible to obtain results regarding the speed of corrosion of the steel reinforcement. Thus, the corrosion potential of the steel reinforcements in concrete is a quantity that indicates a corrosion situation or passive state of these, approximately.

The Pourbaix diagrams that relate pH and potential present the possibility of predicting the conditions under which corrosion, immunity or possibility of passivation

may occur. These representations are valid for a temperature of 25 °C and under a pressure of 1 atm, taking into account the normal hydrogen electrode (NHE). For a better visualization of corrosion, immunity and passivation conditions, a simplified diagram is shown in Figure 7 (GENTIL, 1996).

Through this diagram it is possible to verify the conditions under which corrosion, immunity or possibility of passivation may occur. The immunity region corresponds to the zone where corrosion is thermodynamically unfavorable, that is, the metal is stable. In the passivation region, metal oxides or hydroxides are stable. In the corrosion region there are combinations of pH and potential that indicate that metal ions or complex ions are the stable phases. The dashed lines "a" and "b" delimit the zone where the water is thermodynamically stable. Below the line "a" hydrogen reduction occurs, while above the line "b" there is the evolution of oxygen (GENTIL, 1996).

Figure 7. Simplified Pourbaix Diagram for the Ferro-Água System at 25 °C

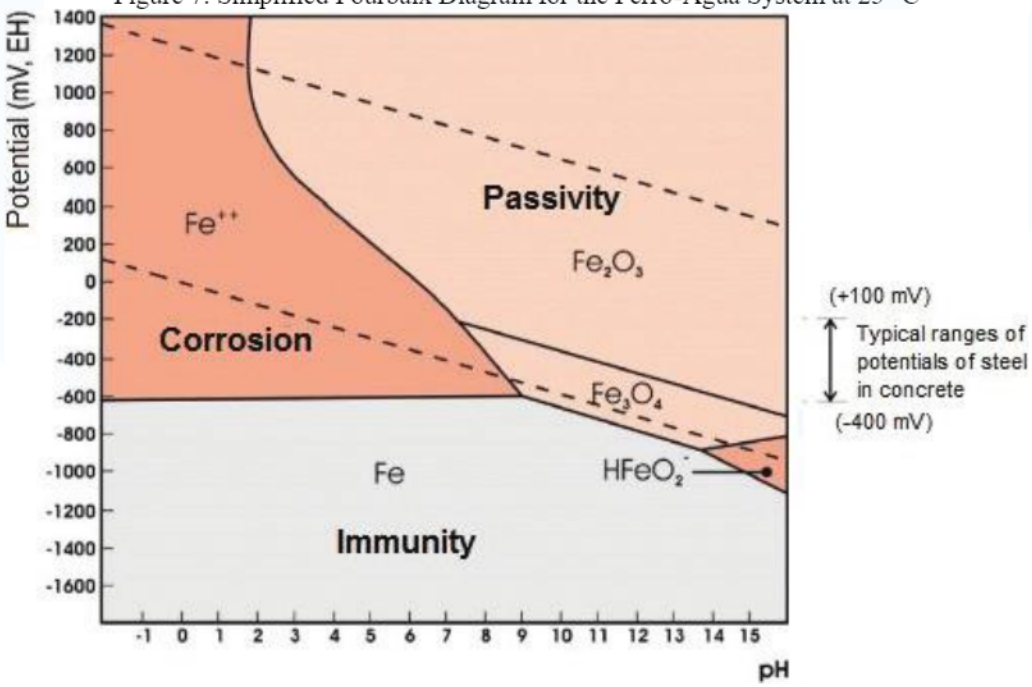

Source: (RIBEIRO et al., 2013)

For the order of magnitude of pH in concrete (between 12.5 and 13.5) and for a usual range of corrosion potential, from +0.1 V to -0.4 V in relation to the standard hydrogen electrode, the electrode reactions verified in iron are passivation. As long as the

pH of the medium is maintained and the passivating film is not destroyed, steel dissolution will not occur and the bars will be protected from corrosion.

The C 876-15 standard presents a correlation between potential intervals and the probability of occurrence of corrosion, taking copper/copper sulfate (Cu/CuSO4, Cu2+) as reference electrode (ASTM, 2015). This correlation, as well as the others, is presented in Table 2.

Table 2. Probability of steel reinforcement corrosion as a function of potential

ELECTRODE TYPE	PROBABILITY OF CORROSION OCCURRING		
	< 10%	10% - 90%	> 90%
STANDARD ELECTRODE OF HYDROGEN (SEH)	> 0,118 V	-0,118 V à -0,032 V	< -0,032 V
CU/CUSO4, CU2+ (ASTM C 876)	> -0,200 V	-0,200 V à -0,350 V	< -0,350 V
HG, HG2CL2, KCL (CALOMELANO)	> -0,124 V	-0,124 V à -0,274 V	< -0,274 V
AG, AGCL/KCL (1M)	> -0,104 V	-0,104 V à -0,254 V	< -0,254 V

Source: ASTM (2015)

According to the theory of mixed potentials, due to polarization phenomena, the corrosion cell tends to achieve a stationary electrochemical state, in which the speed of anodic reactions equals the speed of cathodic reactions, that is, the current densities of both processes are identical (WAGNER; TRAUD, 1938). According to Evans' diagram, shown in Figure 8, the characteristic potential of this state corresponds to the so-called corrosion or mixed potential (Ecorr). It is also observed that this potential is associated with a current density, called corrosion current (icorr).

The most widely used techniques for obtaining the Evans diagram are: the potentiodynamic polarization (CPP), linear polarization resistance (LPR) and scanning linear voltammetry (SLV). These are quantitative tests that allow the instantaneous corrosion rate of a metal to be identified and, by means of measurements, to verify the corrosion rate over a given time (LITTLE; LEE; RAY, 2011). The test procedure is performed by applying a small change in the potential of the steel and checking the change in the existing current and vice-versa.

The technique provides for the continuous scanning of the potential, starting either in the corrosion potential (the one that is established when the material is immersed in the

ISSN: 1696-8352

solution, also called open circuit potential) or in potentials where cathodic reactions predominate (those lower than the corrosion potential), raising the potential at constant scan rate. The scanning speed, the composition of the solution, the immersion time before the potential scan and the test temperature can influence the shape of the polarization curves. The current, in the polarization curves, is shown in absolute values, and is divided by the area of material exposed to the reactions, creating the concept of current density (SEDRIKS, 1986).

Under ideal conditions, a polarization curve (Pc) is the result of an accelerated corrosion experiment in which a metal is polarized in two distinct regions: for potentials more positive than the open potential circuit (OPC) - anodic polarization - and more negative - cathodic polarization. Usually this amplitude is 200 mV to a few volts from the OPC (SRINIVASAN; KANE, 1999). Under certain conditions dissolution can be interrupted by passivation and film formation (CRAMER; B.S. COVINO, JR., 2003; PEREZ, 2004). From the anodic and cathodic polarization curves and the Tafel straight lines, one can analyze the electrochemical system by means of the Evans diagram, as shown in Figure 8 (ZIMER, 2009).

The constant "□" is the charge transfer coefficient, "n" the number of electrons involved in the reaction, R is the universal constant of the gases and T, the temperature. The starting value of the two polarization curves, anodic and cathodic, indicates the corrosion potential of the system (Ecorr).

Figure 8. Representation of the Evans diagram for a metal in solution from the anodic and cathodic polarization curves.

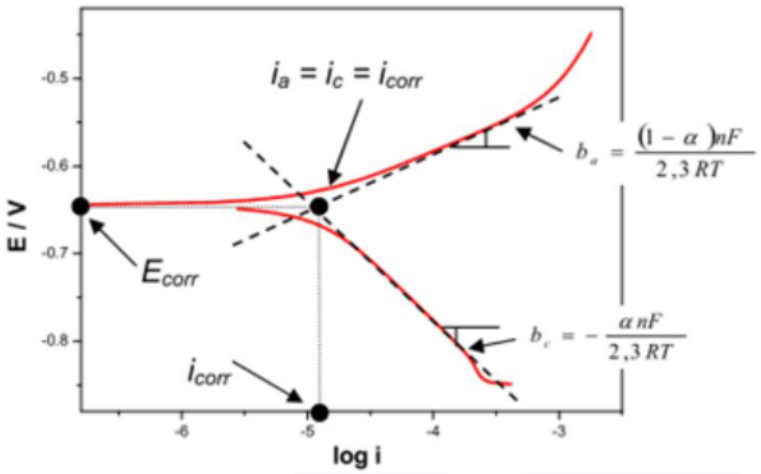

Source: (ZIMER, 2009)

In short, the objective of obtaining the polarization curves is, from the Evans diagram, to obtain direct information about passivation kinetic parameters. The parameters obtained in an electrolyte can be compared to those obtained in another electrolyte when the same electrode is used, knowing that the higher the polarization resistance (Rp), greater is the protection provided by the electrolyte to the electrode. From the Tafel lines can be determined anodic (ba) and cathodic (bc) angular coefficients, which combined, according to Equation 1, will provide the Stern-Gearn coefficient (B).

$$B = \frac{b_a + b_c}{2{,}303 * (b_a + b_c)} \qquad (1)$$

It is worth noting that B varies only between 13 mV and 52 mV for most metal/electrolyte systems analyzed (STERN; WEISERT, 1959), and for concrete steel reinforcement is presented values of B equal to 26 mV for the active state (corrosion) and 52 mV for the passive state (ANDRADE; ALONSO, 1996).

The potential variation ratio (+/- 20 mV or +/- 30 mV), in a given linear stretch, by the voltage variation is called polarization resistance (Rp) (ANDRADE; BUJÁK, 2013; LITTLE; LEE; RAY, 2011). This ratio indicates the resistance to oxidation presented by a material during the application of an external potential. The Rp is inversely

ISSN: 1696-8352

proportional to current density and corrosion rate (ANDRADE; BUJÁK, 2013). From the relation of the coefficient B with the value of the resistance to polarization (Rp) can be found the corrosion current (icorr) related to the said corrosive process, according to Equation 2.

$$i_{corr} = \frac{B}{R_p} \quad (2)$$

As can be seen in Figure 8, the icorr can also be obtained by analyzing the Evans diagram. It is the point where you have the crossing of the tangent lines of cathodic and anodic current. By extrapolating the potential axes, the Ecorr is determined and an indication of the beginning of corrosion is obtained, that is, the potential from which the system will undergo oxidation. It is considered that the steel reinforcement is in corrosion process when icorr > 0,1-0,2 □A/cm2 (ANDRADE; BUJÁK, 2013). From the icorr value one can determine the corrosion velocity (Vcorr) of the system by means of Faraday's Law (GENTIL, 1996), according to Equation 3, where: M is the molar mass of the major constituent of the alloy, in the case of carbon steel it would be the iron; t is the time, in seconds, stipulated for one year; n is the number of electrons involved in the reaction; A is the area, in cm2, of the steel electrode; F is Faraday's constant and d is the density of the alloy, in g/cm3.

$$V_{corr} = \frac{i_{corr} * M * t}{n * A * F * d} \quad (mm/year) \quad (3)$$

The values calculated by Equations 2 and 3 can be compared with Table 3, which relates the current densities with the aggressiveness of the corrosive process (ELSENER et al., 2003).

ISSN: 1696-8352

Table 3. Values of icorr and Vcorr for determination of corrosion aggressiveness

icorr (□A/cm2)	Vcorr (mm/year)	Corrosion level
≤ 0, 1	≤ 0,001	Negligible
0,1 – 0,5	0,001 – 0,005	Low
0,5 – 1,0	0,005 – 0,010	Moderate
> 1, 0	> 0,010	High

Source: ELSENER et al. (2003)

In addition, it is possible to compare the values found in Equation 3 with Table 4 to assign to the system under study, metallic material and corrosive medium, a diagnosis of its corrosion resistance (NACE, 2005).

Table 4. Attribution of corrosion diagnosis by observation of corrosion velocity (Vcorr) of the system

Vcorr calculated		Diagnosis
Uniform corrosion	Pitting corrosion	
Vcorr < 0,025	Vcorr < 0,130	Low Corrosion
0,025 < Vcorr < 0,126	0,130 < Vcorr < 0,200	Moderate corrosion
0,127 < Vcorr < 0,254	0,200 < Vcorr < 0,280	High Corrosion
Vcorr > 0,254	Vcorr > 0,280	Severe Corrosion

Source: NACE (2005)

As a criterion for evaluating the results obtained with the technique, there is a classification based on the icorr found in Table 5 (ALONSO; ANDRADE, 1990).

Table 5. Classification of corrosion degree according to icorr values

icorr (□A/cm2)	Classification
< 0,1 - 0,2	Negligible corrosion
> 0,1 - 0,2	Active corrosion
~ 1,0	Significant, but not severe corrosion
~ 10	Severe corrosion attack

Source: ALONSO; ANDRADE (1990)

The Rp value used in Equation 2 can also be obtained, in practice, by the slope at the point where i=0 in the polarization curve, E versus i, obtained at low scanning speed, on the order of 0.1 mV/s (ASTM, 2014). In addition, it is possible to determine Rp using the electrochemical impedance spectroscopy (EIS) technique, obtaining a response with less experimental error compared to LPR and SLV. EIS is the main spectroscopy technique used for corrosion evaluation of steel immersed in simulated concrete pore solutions, as shown in Figure 9.

Figure 9. Spectroscopies performed on simulated concrete pore solutions used in studies since 2018.

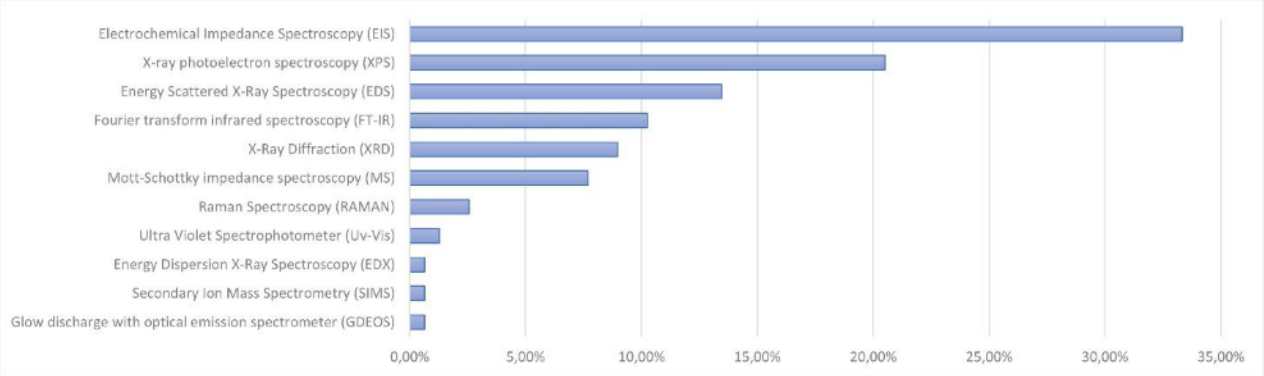

Source: Authors' private collection (May 2023)

Electrochemical impedance spectroscopy (EIS) is a technique used to characterize a wide variety of electrochemical systems and to determine the contribution of individual electrode or electrolyte processes in these systems. It can be used to investigate the dynamics of bound or moving charges in the volume or interface regions of any type of liquid or solid material. The impedance technique assumes that a given electrical circuit, more or less elaborate, can represent the behavior of steel within concrete. (RIBEIRO; SOUZA; ABRANTES, 2015).

Electrochemical impedance spectroscopy (EIS), or AC impedance, is a robust technique where, through the simulation of electrical circuits, with resistors and capacitors, the influence of the components that integrate and are relevant for the study of corrosion in reinforced concrete structures (concrete/ electrolyte, steel/ concrete interface, double electrical layer/ steel) (METHA; MONTEIRO, 2014). EIS has an advantage over LPR, as it suffers less influence and alteration of the results by external interference, besides being able to detect corrosion rates below 10-4 mm/year (SILVERMAN, 2011).

The equivalent electrical models, obtained based on the Impedance Spectroscopy technique, normally generate circuits of type R-C (Resistance - Capacitance). The EIS technique is standardized by ASTM G-106 (COMMITTEE, 2010). Because the analyzed samples do not present an ideal capacitance, a calibration is required for R-CPE models (Resistance - Constant phase element).

ISSN: 1696-8352

In a study on the corrosion inhibition efficiency of carbon steel, in SCP, using compound nitrite with sodium D-gluconate it was possible to verify, through the graphs of Nyquist and Bode, that after adding the corrosion inhibitor, the impedance arc radius in the Nyquist diagram increased greatly and the curve slope in the low frequency region increased, as illustrated in Figure 10 (XU et al., 2021).

Figure 10. Nyquist graph of carbon steel electrode with different levels of corrosion inhibitor

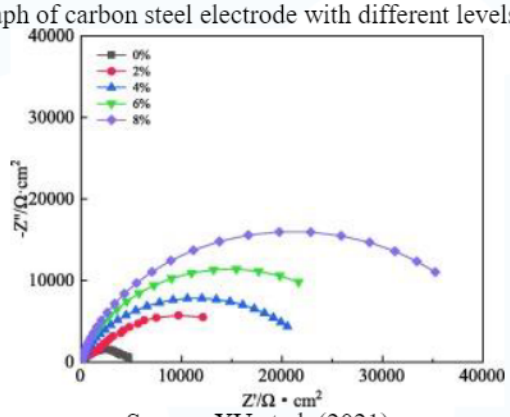

Source: XU et al. (2021)

The efficiency of the protective layer becomes more evident with the increase of the concentration of the nitrite compound with sodium D-gluconate, and works mainly through the cathodic electrochemical process that inhibits the corrosion of steel bars (KORNBLUM; BLACKWOOD; MOOBERRY, 1956; YANG et al., 2012). Figure 11 shows that the low frequency impedance value and the maximum phase angle increased with the corrosion inhibitor (XU et al., 2021). This indicates that the addition of corrosion inhibitor improved the corrosion resistance of carbon steel by promoting the formation of a more stable protective film on the surface, which prevented chloride and oxygen ions from hitting the surface of carbon steel.

ISSN: 1696-8352

Figure 11. Bode graph of carbon steel electrode with different levels of corrosion inhibitor.

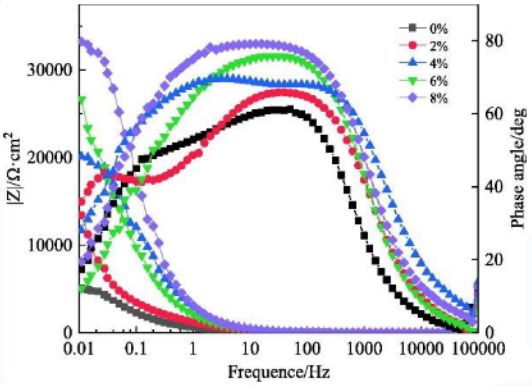

Source: XU et al. (2021)

To quantitatively analyze carbon steel corrosion, the equivalent circuit, illustrated in Figure 12, was used to describe the Nyquist charts (XU et al., 2021). This equivalent circuit was also used by other researchers to model the electrochemical behavior of carbon steel in alkaline médium (ZHAO, Y et al., 2019). In the equivalent circuit, Rs is the resistance of the solution; Rf is the film resistance; Rct is the charge transfer resistance, which reflects the electron transfer difficulty between the anode dissolution and depolarizer reduction; the Cf is the capacitance of the film and the dispersion index a1 constitutes the constant phase angle elemento CPE1; the capacitance of double electrical layer Cdl and the dispersion index a2, constitute the constant phase angle element CPE2.

Figure 12. Equivalent circuit

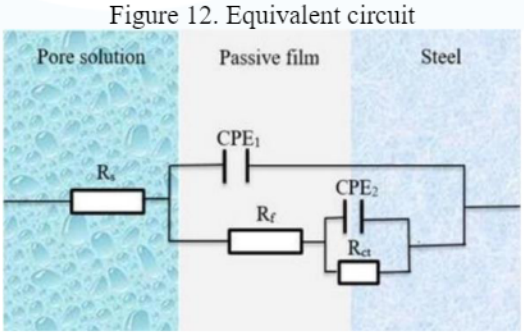

Source: XU et al. (2021)

According to the results found by Xu, et al (2021), in addition to the load transfer resistance Rt, the influence of the protective film on carbon steel can be described by Cdl (FENG et al., 2017; SAHOO; BALASUBRAMANIAM, 2008). The capacitance of the

ISSN: 1696-8352

electric double layer (CPE2) of the solution with corrosion inhibitor was significantly lower than that of the solution without corrosion inhibitor (YANG et al., 2019). According to the Helmholtz model (BOMMERSBACH et al., 2005), the double layer capacitance Cdl can be expressed by Equation 4, where "S" is the surface area of the working electrode, "d" represents the thickness of the double layer, e0 and ε are dielectric vacuum and film constants, respectively.

$$C_{dl} = \frac{\varepsilon_0 * \varepsilon}{d} * S \quad (4)$$

The dielectric constant of water molecules is greater than that of the corrosion inhibitor. When water molecules at the steel/solution interface are replaced by corrosion inhibitors, the capacitance of the solution composed of corrosion inhibitor molecules is significantly lower than that of water molecules, so, Cdl decreases. According to Equation 4, the thickness of the double layer increases with the content of the corrosion inhibitor in the SCP, which indicates that the corrosion inhibitor adsorbed to form a film on the surface of the carbon steel, which blocked the penetration of aggressive ions (XU et al., 2021).

It was also calculated the inhibition efficiency (□) of the corrosion inhibitor, with different concentrations, using Equation 5, where Rct and R'ct efer to the charge transfer resistance of the electrode in SPC without and with corrosion inhibitor, in ohm (□).

$$\eta = \frac{R'_{ct} - R_{ct}}{R'_{ct}} \quad (5)$$

In the study in question, the resistance to charge transfer, Rct and the resistance of Rf film increased after the addition of corrosion inhibitor, implying that the passive film became more stable and resistant. When the inhibitor concentration increased from 2% to 8%, there was an increase in resistance efficiency from 60.73% to 89.96%. The higher inhibitor concentration helped increase the adsorption of the nitrite corrosion inhibitor compound with sodium D-gluconate on the surface of the steel bar and formed

a complete and compact adsorption film to improve the resistance to chloride ions (XU et al., 2021).

In another study the influence of calcium ion in the solution of concrete pores on the passivation of galvanized steel bars was evaluated. They were performed after 264 h of immersion when the potential and polarization resistance were both stationary, in order to define the passive state of the galvanized steel surface (ZHENG et al., 2018). To analyze the EIS results, the surface models and equivalent circuit graphs were established as in figure 13.

According to the results of the linear polarization resistance test and observation of the sample surface in the saturated solution of Ca(OH)2, this was covered by a compact layer of calcium hydroxyzincate (CHZ) with a rough surface exhibiting a high value of resistance to polarization, can be simulated by the model of figure 13(a).The surface of the samples in cement and water solution (ECP), which were covered by porous or loose layers of corrosion products and exhibited lower polarization resistance values, can be simulated by the figure 13(b). The surfaces of the specimens that were covered by a compact layer of Zn(OH)2 and exhibited higher polarization resistance value, can be simulated by 13(c). The samples in which there was little corrosion product observed, exhibited low values of resistance to polarization, therefore, the system could be simulated by the modelo of figure 13(d).

In the equivalent circuit graphics, Rs represents the electrolyte resistance between the working electrode and the reference electrode; Rf is the resistance of the corrosion product layer formed on the surface of the galvanized coating; Rpore the resistance of the alveolar pores on the surface or passive film; Rct the resistance of the alveolar pores on the surface or passive film; Rct represents the charge transfer resistance; Q denotes the constant phase element (CPE) representative of the double electrical layer formed at the steel-concrete interface when its immersion in electrolyte (LI et al., 2016). Qf and Qdl represent the capacitance of the corrosion products layer on the surface of the galvanized steel and the capacitance of the electric double layer respectively (LI et al., 2011; TIAN et al., 2015).

ISSN: 1696-8352

Thus, to work with capacitance values, it is necessary to convert the CPE into a pseudo-capacitance, which can be equated as through an impedance or admittance. . The equation for impedance considering a CPE is presented in Equation 6. Where ZCPE is the impedance of the constant phase element (Ohm.cm2), w is the angular frequency of AC alternating voltage (rad/s), Y0 is the admittance of the CPE (Ohm.cm-2.s-α), and α the exponential term, which represents the ease of diffusion of ions in the passivation film (DIARD; LE GORREC; MONTELLA, 2013).

$$Z_{CPE} = \frac{1}{Y_0 * (j * \omega)^{\alpha}} \quad (6)$$

Figure 13. Surface models of the galvanized steel in the simulated solutions after 264 h of immersion and the equivalent circuits used to adjust the results.

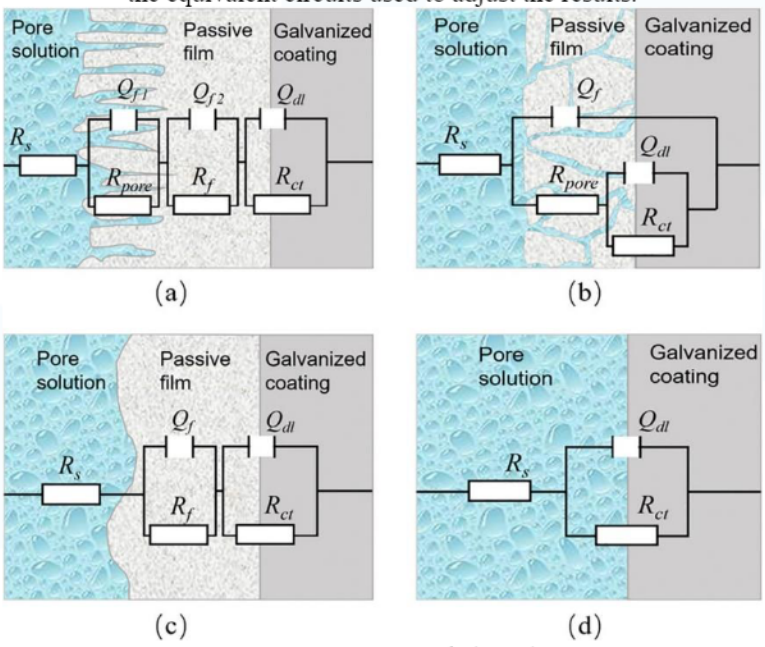

Source: ZHENG et al. (2018)

The parameter "□" is directly related to the microstructure, roughness and irregularity existing on the electrode surface, ranging from 0 to 1, with values closer to 1 indicating an ideal capacitive behavior (KATIYAR; RANDHAWA, 2019), while "□" close to 0.5 indicam that or CPE is becoming a component of Warburg (RETTER et al., 2003). In other words, when "□" is 1, the element is a capacitor, since when the behavior

ISSN: 1696-8352

is governed by a process of mass transfer, "□" approaches 0.5, and intermediate values of "□" relate to the non-homogeneity and surface roughness of the electrode (MACDONALD, 1987).

In addition to the kinetic characteristics of the corrosive process, EIS allows to identify whether corrosion occurs in a generalized or localized way, and it is also possible, through the adaptation of the proposed electrical circuit, to estimate the average thickness of the passivation film (CASCUDO, 1997). As the technique allows separating the elements that compose the electrochemical cell in different electrical components, it is possible to identify the electrical characteristics of the solution and the steel/solution interface [84,85]. The analysis of the results is done through the individual evaluation of each of the parameters of the proposed electric circuit, and also through Nyquist graphs, according to Figure 14, and Bode graphs, where it is possible to analyze the influence of the sample components (CASCUDO, 1997).

Figure 14. Representation of the Nyquist diagram

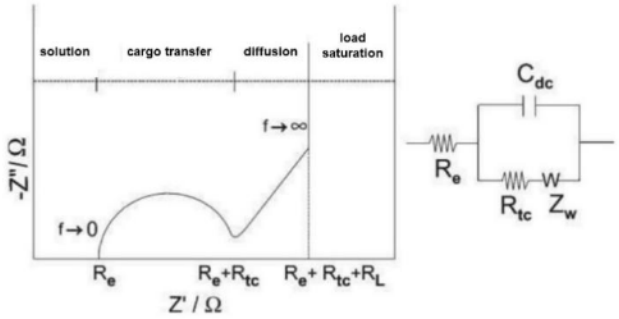

Source: adapted (CASCUDO, 1997)

In parallel impedance measurements some techniques can be employed, such as: scanning electron microscopy (SEM) to determine the morphology; microanalysis by EDS as a technique to determine the local chemical composition; and X-ray diffraction as a technique to determine the phases of corrosion products (FeS2 film, for example) These techniques allow a better understanding of the ex situ corrosion process and can serve as feedback for future assignments of equivalent circuits for impedance measurements. SEM is the main image analysis technique used for corrosion evaluation of steel immersed in simulated concrete pore solutions, as illustrated in Figure 15.

Figure 15. Image analysis performed on simulated concrete pore solutions used in studies since 2018.

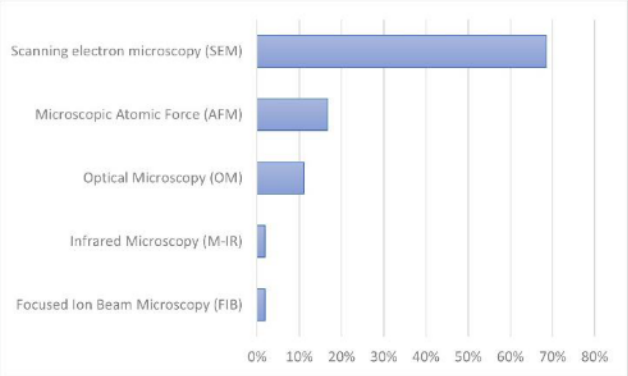

Source: Authors' private collection (May 2023)

The scanning electron microscopy technique (SEM) is an effective tool for the characterization of surface morphology, as it allows the increase of up to 50 thousand times. It consists in scanning the sample with an electron beam, causing the emission of secondary electrons that are used in the formation of the image to be analyzed (CALLISTER; RETHWISCH, 2002).

When the SEM is coupled with equipment capable of performing energy dispersive X-ray spectroscopy (EDS), a point of the image obtained by the microscope is chosen and, through the emission of rays-X in the sample and, with the interpretation of the characteristic return energy of each element, it is possible to say the elements present in the sample. It is also possible to perform a mapping of a SEM image by coloring each element with a specific color, so that it is possible to know where the elements are concentrated in the sample.

SEM was used to investigate and characterize the passive films formed during 5 days of immersion of carbon steel electrodes in reference solution (SCP) and solution with corrosion inhibitor based on sugarcane ash sand (SBAS) (GROMBONI et al., 2021). Figure 16 illustrates the SEM images of the working electrode surfaces.

The passivation products are already visible in Figure 16 (A) and (E), where the defects formed by the polishing process become undetectable as the passivating layer formation process occurs. Rod-shaped precipitates are clearly observed in Figure 16 (B) and (F), which grow at the edge when the amount of precipitate increases with immersion time, leading to a globular structure, starting from the third day, as illustrated in Figure

16 (C) and (G). As seen in the micrographs, the steel surface immersed in the SBAS medium shows a higher total coverage than in the REF medium. This behavior is more evident in the final monitoring period, as per Figure 16 (D), where there is a completely covered surface (GROMBONI et al., 2021).

Figure 16. SEM images of the working electrode surfaces after different numbers of days of immersion

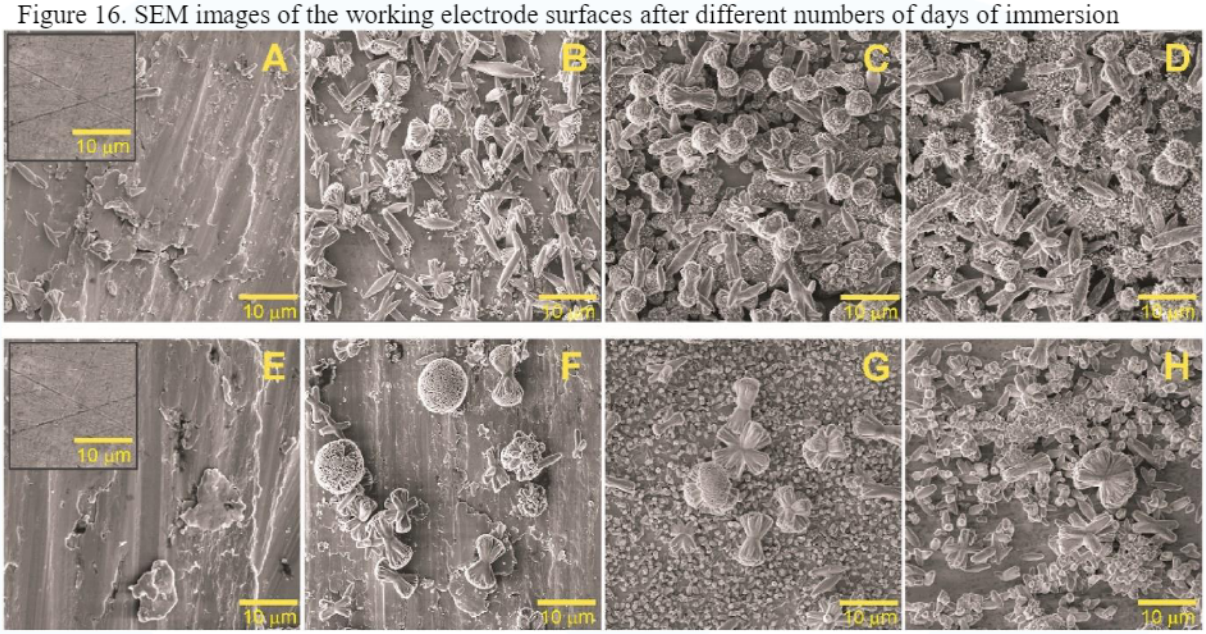

Source: (GROMBONI et al., 2021)

A possible explanation for precipitate formation comes from the local pH variation at the steel/solution interface. It is well known that the formation of passive films (iron oxides and hydroxides) promotes a local pH decrease, causing a pH shift of up to 3 units according to some authors (SILVA et al., 2016). In solutions containing large amounts of calcium hydroxides, as is the case of the solutions investigated here, an important decrease in the solubility of CaCO3 could reasonably explain the precipitation of such compounds in the passivated steel.

SEM was used to characterize the surface morphology of super hydrophobic low carbon steel (SHLCS) and low carbon steel (LCS) in a study on the chloride corrosion resistance of double-layer anti-corrosion coating. The elemental composition of the surface after being immersed in SPC containing 3.5% by weight chloride for 4 days was measured by EDS (QU et al., 2021). Three different modification methods were used to

ISSN: 1696-8352

reduce the surface energy of the rough structure by obtaining a super hydrophobic surface: 1) the LCS surface deposited with Zn/Ag was heated to 100 °C for 1 h (SHLCS-H); 2) the LCS surface deposited with Zn/Ag was soaked in 0.02 M stearic acid ethanol solution for 12 h and then air-dried (SHLCS-STA) and; 3) the LCS surface deposited with Zn/Ag was soaked in an ethanol solution of stearic acid 0,02 M for 12 h and then heated to 100 °C for 1 h, to form the super hydrophobic surface (SHLCS-STA&H).

Figure 17 shows the surface of the LCS after immersion, and spherical rust can be seen in the micrograph, which is a typical feature of goethite (α - FeOOH) (TIAN et al., 2019). At the same time, it is verified in the results of the EDS analysis, in Figure 17(a) that there is chlorine on the surface of the LCS. Furthermore, it can be seen in Figure 17 (b) and (c) that there are other substances adhered to the surface of SHLCS-H and SHLCS-STA from SCP. The EDS analysis in Figure 17 (b) and (c) finds the presence of Cl, K, Ca, Na and other substances. The SEM images and EDS analysis results of SHLCS-H and SHLCS-STA show that the superhydrophobic effects on the surface of the two samples disappear, causing the substances on the SCP to attach to the surface of the samples. However, the SHLCS-STA and SHLCS-H surface still maintain good roughness, as shown in Figure 17 (b) and (c) (QU et al., 2021).

The disappearance of the superhydrophobicity may be due to the loss of low surface energy functional groups on the surface of the structure. Although the superhydrophobic effects of the SHLCS-STA and SHLCS-H surfaces are disappearing, no obvious corrosion traces are observed in the SEM images. This may occur because the rough surface structure and the inner Zn coating may also protect the inner LCS substrate. The surface morphology of SHLCS-STA&H, illustrated in Figure 17 (d), after being immersed for 4 d is not significantly different from that before being immersed. The EDS analysis results also show no chloride and other substances from the pore solution, which indicates that the surface of SHLCS-STA&H is still superhydrophobic (QU et al., 2021).

Figure 17. SEM micrographs and EDS element analysis results of LCS and SHLCS samples after exposure to simulated concrete pore solution containing 3.5% by weight NaCl for 4 days.

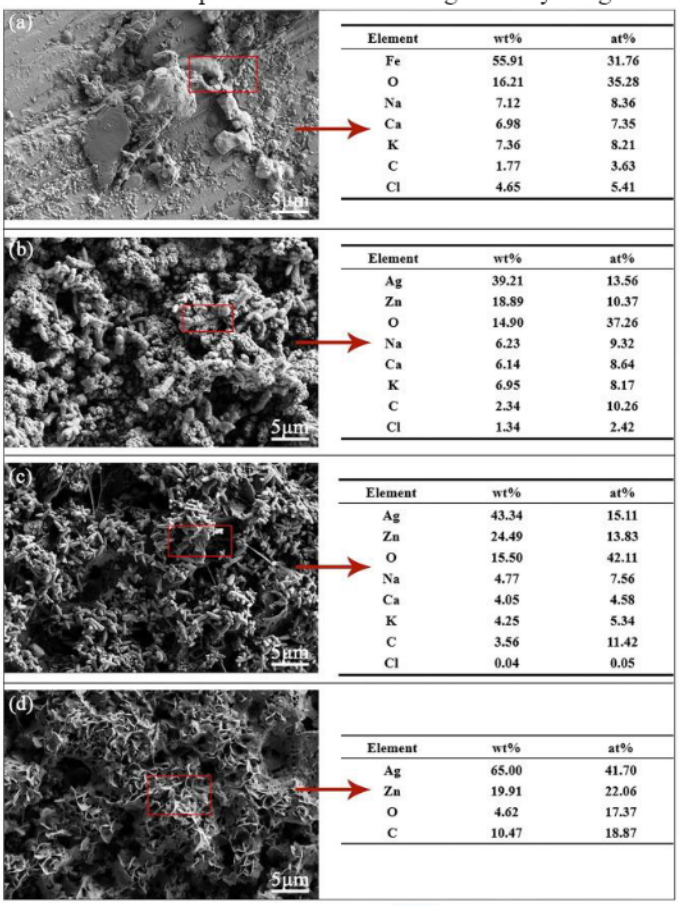

Element	wt%	at%
Fe	55.91	31.76
O	16.21	35.28
Na	7.12	8.36
Ca	6.98	7.35
K	7.36	8.21
C	1.77	3.63
Cl	4.65	5.41

Element	wt%	at%
Ag	39.21	13.56
Zn	18.89	10.37
O	14.90	37.26
Na	6.23	9.32
Ca	6.14	8.64
K	6.95	8.17
C	2.34	10.26
Cl	1.34	2.42

Element	wt%	at%
Ag	43.34	15.11
Zn	24.49	13.83
O	15.50	42.11
Na	4.77	7.56
Ca	4.05	4.58
K	4.25	5.34
C	3.56	11.42
Cl	0.04	0.05

Element	wt%	at%
Ag	65.00	41.70
Zn	19.91	22.06
O	4.62	17.37
C	10.47	18.87

Source: (QU et al., 2021)

In this study, in particular, SHLCS-STA&H showed better corrosion resistance than other samples (SHLCS-STA, SHLCS-H and LCS), with a 97.1% corrosion protection. After immersing the sample in simulated 4 d concrete pore solution, SHLCS-STA&H still maintained the super-hydrophobic property. The double anti-corrosion strategy of the Zn layer and the super-hydrophobic layer significantly improved the anticorrosive efficiency of carbon steel in the simulated solution of concrete pores.

4 CONCLUSION

The systematic review showed that the use of simulated concrete pore solutions (SCP) has gained space in the scientific world, especially with regard to the study of corrosion of steel rebar, because this solution allows simulating, in the environment of an

ISSN: 1696-8352

electrochemical cell, accelerated corrosion, which makes it possible to quickly assess what happens to steel rebar when immersed in concrete as a function of time, in addition to the possibility of simulating attacks such as the maritime environment and carbonation.

However, the use of SCP composed only of saturated calcium hydroxide, even being widely used, is not enough to simulate the content of what is actually present in the pores of concrete, because the only corrosion inhibitor is the concentration of hydroxyl, which determines the limit of chlorides to initiate steel corrosion.

Therefore, the use of an SPC composed by the mixture of cement and water better represents the reality, due to the hydration of the Portland cement contain a series of ions (Na+ , K+ , Ca2, Mg2+, Al2+ and (SO4)2-), the chlorine ions are physically adsorbed by the CSH (hydrated silicate) and C3A (tricalcium aluminate) chemically binds chlorides to produce Friedel salt (C3A.CaCl2.10H2O), which guarantees steel a lower risk of corrosion, as it promotes the removal of a portion of the chlorine ions from the solution.

OCP monitoring is a widely used electrochemical technique to evaluate the formation of passivating oxide films or corrosive oxides on a metal. However, this technique indicates only the balance between the anodic and cathodic reaction, without offering quantitative information, therefore, it is not possible to obtain results regarding the speed of corrosion of the rebar, being, the corrosion potential of the reinforcements in the concrete a quantity that indicates a corrosion situation or passive state of these, in an approximate way.

The techniques used to obtain the Evans diagram, are quantitative tests, which allow to identify the instantaneous corrosion rate of a metal and, through measurements, to verify the corrosion rate in a given time, The objective of obtaining the polarization curve is to have information on kinetic parameters of passivation, such as corrosion potential (Ecorr), using Tafel, polarization resistance (Rp), corrosion current (icorr) and corrosion speed (Vcorr).

The techniques most used to do such analysis are the Linear Polarization Resistance (LPR) and Linear Voltammetry (LSV), but it is also possible to obtain with response, with less experimental error, using electrochemical impedance spectroscopy (EIS).

ISSN: 1696-8352

With the EIS technique, for the steel/concrete system, it is possible to obtain information on various parameters, such as the presence of surface films, concrete characteristics, interfacial corrosion and mass transfer phenomena. However, the interpretation of the results can be a difficult task, and the need for an equivalent circuit, which can change according to steel conditions, makes the technique more acceptable for laboratory studies.

The main advantages of this technique are: 1. Provides information on the kinetics of the process, by the speed of corrosion; 2. Accuracy and reproducibility, suitable for high resistivity environments such as concrete; 3. Provide data on the electrochemical control mechanism, indicating whether the corrosive process occurs by activation, concentration or diffusion; 4. Characterize the steel reinforcement state and corrosion morphology; 5. Be non-destructive and non-disruptive, since signals applied are of small amplitude, so that the corrosion potential is not changed; 6. Allow the monitoring of the evolution of the passive or active state over time.

Given the above, it is evident that for the use of solutions that simulate the pores of concrete the ideal is to use water/cement ratios that allow the filtration and dissolution of ions in solution, so that it is possible to apply electrochemical techniques obtaining a result as close as possible to reality.

ACKNOWLEDGMENTS

The authors would like to thank the Network of Biodiversity and Biotechnology of the Legal Amazon (BIONORTE) and the Coordination of Improvement of Higher Education Personnel (CAPES) for supporting the work.

ISSN: 1696-8352

REFERENCES

ALONSO, C.; ANDRADE, C. Effect of nitrite as a corrosion inhibitor in contaminated and chloride-free carbonated mortar. Materials Journal, [s. l.], v. 87, n. 2, p. 130–137, 1990.

ANDRADE, C.; ALONSO, C. Corrosion rate monitoring in the laboratory and on-site. Construction and building materials, [s. l.], v. 10, n. 5, p. 315–328, 1996.

ANDRADE, C.; BUJÁK, R. Effects of some mineral additions to Portland cement on reinforcement corrosion. Cement and Concrete Research, [s. l.], v. 53, p. 59–67, 2013. Disponível em: http://dx.doi.org/10.1016/j.cemconres.2013.06.004.

ASTM, C. C876 - Standard test method for corrosion potentials of uncoated reinforcing steel in concrete. ASTM International: West Conshohocken, West Conshohocken, PA, USA, 2015.

ASTM, G. G 59-Standard test method for conducting potentiodynamic polarization resistance measurements. [S. l.: s. n.], 2014.

BAKKER, R. F. M. Corrosion of stell in concrete. London: [s. n.], 1988.

BEN MANSOUR, H.; DHOUIBI, L.; IDRISSI, H. Effect of Phosphate-based inhibitor on prestressing tendons corrosion in simulated concrete pore solution contaminated by chloride ions. Construction and Building Materials, [s. l.], v. 171, p. 250–260, 2018. Disponível em: https://doi.org/10.1016/j.conbuildmat.2018.03.118.

BOLINA, F. L.; TUTIKIAN, B. F.; HELENE, P. Patologia de estruturas. [S. l.]: Oficina de Textos, 2019.

BOMMERSBACH, P. et al. Formation and behaviour study of an environment-friendly corrosion inhibitor by electrochemical methods. Electrochimica Acta, [s. l.], v. 51, n. 6, p. 1076–1084, 2005.

CALLISTER, W. D.; RETHWISCH, D. G. Ciência e Engenharia de Materiais: uma introdução. Rio de Janeiro: LTC, 2002. v. 589

CASCUDO, O. O controle da corrosão de Armaduras de Concreto Armado. Goiânia: Editora PINI, 1997.

CHEN, M. et al. Novel Ca-SLS-LDH nanocomposites obtained via lignosulfonate modification for corrosion protection of steel bars in simulated concrete pore solution. Applied Clay Science, [s. l.], v. 211, n. June, p. 106195, 2021. Disponível em: https://doi.org/10.1016/j.clay.2021.106195.

COMMITTEE, G. G106 - Practice for Verification of Algorithm and Equipment for Electrochemical Impedance Measurements. ASTM International, [s. l.], 2010.

CRAMER, S. D.; B.S. COVINO, JR., E. Corrosion: Fundamentals, Testing, and Protection. Journal of Thermal Spray Technology, [s. l.], v. 12, n. 4, p. 459–463, 2003.

ISSN: 1696-8352

DIARD, J. P.; LE GORREC, B.; MONTELLA, C. Handbook of Electrochemical Impedance Spectroscopy-Electrical Circuits containing CPEs. Bio-logic Science Instruments, [s. l.], 2013.

ELSENER, B. et al. Half-cell potential measurements—Potential mapping on reinforced concrete structures. Materials and Structures, New York, v. 36, n. 7, p. 461–471, 2003.

FENG, X. et al. The corrosion inhibition efficiency of aluminum tripolyphosphate on carbon steel in carbonated concrete pore solution. Corrosion Science, [s. l.], v. 124, p. 150–159, 2017.

GENTIL, V. Corrosão. Rio de Janeiro: LTC-Livros Técnicos e Científicos Editora SA, 1996.

GROMBONI, M. F. et al. Impact of agro-industrial waste on steel corrosion susceptibility in media simulating concrete pore solutions. Journal of Cleaner Production, [s. l.], v. 284, p. 124697, 2021. Disponível em: https://doi.org/10.1016/j.jclepro.2020.124697.

GU, G. P.; BEAUDOIN, J. J.; RAMACHANDRAN, V. S. Techniques for corrosion investigation in reinforced concrete. New York: William Andrew Publishing, 2001.

HELENE, P.; ANDRADE, T. Concreto de cimento Portland. São Paulo: IBRACON, 2007.

HOU, B.; LI, X.; CHEN, G. The Roles of Input Matrix and Nodal Dynamics in Network Controllability. IEEE Transactions on Control of Network Systems, [s. l.], v. 5, n. 4, p. 1764–1774, 2018.

JIANG, L. et al. Influence of chloride salt type on threshold level of reinforcement corrosion in simulated concrete pore solutions. Construction and Building Materials, [s. l.], v. 30, p. 516–521, 2012. Disponível em: http://dx.doi.org/10.1016/j.conbuildmat.2011.12.044.

KAPAT, C.; PRADHAN, B.; BHATTACHARJEE, B. Potentiostatic study of reinforcing steel in chloride contaminated concrete powder solution extracts. Corrosion Science, [s. l.], v. 48, n. 7, p. 1757–1769, 2006.

KATIYAR, P. K.; RANDHAWA, N. S. Corrosion behavior of WC-Co tool bits in simulated (concrete , soil , and mine) solutions with and without chloride additions. International Journal of Refractory Metals & Hard Materials, [s. l.], v. 85, n. July, p. 105062, 2019. Disponível em: https://doi.org/10.1016/j.ijrmhm.2019.105062.

KEMPL, J.; ÇOPUROGLU, O. The interaction of pH, pore solution composition and solid phase composition of carbonated blast furnace slag cement paste activated with aqueous sodium monofluorophosphate. 15th Euroseminar on Microscopy Applied to Building Materials, [s. l.], n. June 2015, p. 287–296, 2015.

KOCH, G. Cost of corrosion. In: TRENDS IN OIL AND GAS CORROSION RESEARCH AND TECHNOLOGIES: PRODUCTION AND TRANSMISSION. [S. l.]: Elsevier Ltd, 2017. p. 3–30.

KORNBLUM, N.; BLACKWOOD, R. K.; MOOBERRY, D. D. The Reaction of Aliphatic Nitro Compounds with Nitrite Esters1, 2. Journal of the American Chemical Society, [s. l.], v. 78, n. 7, p. 1501–1504, 1956.

KULAKOWSKI, M. P. Contribuição ao estudo da carbonatação em concretos e argamassas compostos com adição de sílica ativa. 2002. 199 f. - LUME - Repositório Digital, Porto Alegre, 2002.

L.T. MAMMOLITI, L. C.; BROWN, C. M. H.; HOPE, B. B. The influence of surface finish of reinforcing steel and pH of the test solution on the chloride threshold concentration for corrosion initiation in synthetic pore solution. Cement and Concrete Research, [s. l.], v. 26, n. December, p. 545–550, 1996.

LI, J. et al. Effect of heat treatment on corrosion behavior of AZ63 magnesium alloy in 3.5 wt.% sodium chloride solution. Corrosion Science, [s. l.], v. 111, p. 288–301, 2016.

LI, W. et al. Effects of two fungicides on the corrosion resistance of copper in 3 . 5 % NaCl solution under various conditions. Corrosion Science, [s. l.], v. 53, n. 2, p. 735–745, 2011. Disponível em: http://dx.doi.org/10.1016/j.corsci.2010.11.006.

LITTLE, B. J.; LEE, J. S.; RAY, R. I. Diagnosing, measuring and monitoring microbiologically influenced corrosion (MIC) (J. W. e Sons, Org.). Ontario, EUA: REVIE, R. W., 2011.

LIU, J. Z. et al. Corrosion behavior of carbon steel in chloride contaminated simulated concrete pore solution with carboxylate of benzoic acid and dimethylethanolamine. Anti-Corrosion Methods and Materials, [s. l.], v. 64, n. 5, p. 555–562, 2017.

LONGUET, P. La phase liquide du ciment hydraté. Revue des Materiaux de constructions, [s. l.], v. 676, p. 35–41, 1973.

MACDONALD, J. R. Impedence Spectroscopy--Emphasizing Solid Materials and Systems. Wiley-Interscience, John Wiley and Sons, [s. l.], p. 1–346, 1987.

MANDAL, S. et al. Ammonium phosphate as inhibitor to mitigate the corrosion of steel rebar in chloride contaminated concrete pore solution. Molecules, [s. l.], v. 25, n. 17, 2020.

METHA, P. K.; MONTEIRO, P. J. M. Concreto: microestrutura, propriedades e materiais. São Paulo: IBRACON, 2014. v. 2

MOHER, D. et al. Preferred reporting items for systematic review and meta-analysis protocols (PRISMA-P) 2015 statement. Systematic reviews, [s. l.], v. 4, n. 1, p. 1–9, 2015.

NACE. Standard recommended practice: preparation, installation, analysis, and interpretation of corrosion coupons in oilfield operations. [S. l.]: NACE, 2005.

O'CONNOR, A.; SARGEANT, J.; WOOD, H. Systematic reviews. Veterinary Epidemiology, [s. l.], p. 397–420, 2017.

ISSN: 1696-8352

OGUNSANYA, I. G.; HANSSON, C. M. Influence of chloride and sulphate anions on the electronic and electrochemical properties of passive films formed on steel reinforcing bars. Materialia, [s. l.], v. 8, p. 100491, 2019.

ORTOLAN, V. de K. Avaliação da influência do pH e da força iônica da solução dos poros do concreto na resistência à corrosão da armadura. 2015. 128 f. - Unisinos, São Leopoldo, 2015.

PACHECO-TORGAL, F. et al. Biotechnologies and biomimetics for civil engineering. Biotechnologies and Biomimetics for Civil Engineering, [s. l.], p. 1–437, 2015.

PENG, Y. et al. Effect of simulated pore solution on passivation characteristic of P110 steel. Journal of Petroleum Science and Engineering, [s. l.], v. 167, n. March, p. 949–956, 2018. Disponível em: https://doi.org/10.1016/j.petrol.2018.03.009.

PEREZ, N. Electrochemistry and corrosion science. Kluwer Academic publishers, [s. l.], p. 189–246, 2004.

PLUSQUELLEC, G. et al. Determination of the pH and the free alkali metal content in the pore solution of concrete: Review and experimental comparison. Cement and Concrete Research, [s. l.], v. 96, p. 13–26, 2017.

POSSAN, E. et al. CO2 uptake potential due to concrete carbonation: A case study. Case Studies in Construction Materials, [s. l.], v. 6, p. 147–161, 2017. Disponível em: http://dx.doi.org/10.1016/j.cscm.2017.01.007.

POURSAEE, A. Corrosion of steel bars in saturated Ca(OH)2 and concrete pore solution. Concrete Research Letters, [s. l.], v. 1, n. 3, p. 90–97, 2010.

POURSAEE, A.; ANGST, U. M. Principles of corrosion of steel in concrete structures. In: CORROSION OF STEEL IN CONCRETE STRUCTURES. [S. l.]: Elsevier Ltd, 2023. p. 17–34.

PRADHAN, B.; BHATTACHARJEE, B. Corrosion zones of rebar in chloride contaminated concrete through potentiostatic study in concrete powder solution extracts. Corrosion Science, [s. l.], v. 49, n. 10, p. 3935–3952, 2007.

QU, L. et al. Chloride corrosion resistance of double-layer anticorrosive coating in simulated concrete pore solution. Construction and Building Materials, [s. l.], v. 295, p. 123682, 2021. Disponível em: https://doi.org/10.1016/j.conbuildmat.2021.123682.

RANI, B. E. A.; BASU, B. B. J. Green inhibitors for corrosion protection of metals and alloys: An overview. International Journal of Corrosion, [s. l.], v. 2012, n. 6, p. 16–25, 2012.

RETTER, U. et al. On the impedance of potassium nickel (II) hexacyanoferrate (II) composite electrodes * the generalization of the Randles model referring to inhomogeneous electrode materials. Journal of Electroanalytical Chemistry, [s. l.], v. 546, p. 87–96, 2003.

ISSN: 1696-8352

RIBEIRO, D. V. et al. Corrosão em Estruturas de Concreto Armado: Teoria, Controle e Métodos de Análise. São Paulo: Elsevier, 2013. v. 1

RIBEIRO, D. V.; SOUZA, C. A. C.; ABRANTES, J. C. C. Uso da Espectroscopia de Impedância Eletroquímica (EIE) para monitoramento da corrosão em concreto armado. Revista IBRACON de Estruturas e Materiais, [s. l.], v. 8, p. 529–546, 2015.

SAHOO, G.; BALASUBRAMANIAM, R. On the corrosion behaviour of phosphoric irons in simulated concrete pore solution. Corrosion Science, [s. l.], v. 50, n. 1, p. 131–143, 2008.

SCOTT, A.; ALEXANDRE, M. G. Effect of supplementary cementitious materials (binder type) on the pore solution chemistry and the corrosion of steel in alkaline environments. Cement and Concrete Research, [s. l.], v. 89, p. 45–55, 2016.

SEDRIKS, A. J. Effects of Alloy Composition and Microstructure on the Passivity of Stainless Steels. Corrosion, [s. l.], v. 42, n. 7, p. 376–389, 1986.

SHAHEEN, F.; PRADHAN, B. Influence of sulfate ion and associated cation type on steel reinforcement corrosion in concrete powder aqueous solution in the presence of chloride ions. Cement and Concrete Research, [s. l.], v. 91, p. 73–86, 2017.

SHI, J. et al. Improved corrosion resistance of a new 6% Cr steel in simulated concrete pore solution contaminated by chlorides. Corrosion Science, [s. l.], v. 174, 2020.

SHI, J. et al. Role of red mud in natural passivation and chloride-induced depassivation of reinforcing steels in alkaline concrete pore solutions. Corrosion Science, [s. l.], v. 190, n. June, p. 109669, 2021. Disponível em: https://doi.org/10.1016/j.corsci.2021.109669.

SILVA, M. M. et al. Near-surface solution pH measurements during the pitting corrosion of AISI 1020 steel using a ring-shaped sensor. Journal of Electroanalytical Chemistry, [s. l.], v. 780, p. 379–385, 2016.

SILVERMAN, D. C. Practical corrosion prediction using electrochemical techniques. Uhlig's Corrosion Handbook, [s. l.], p. 1129–1166, 2011.

SOUZA, R. H. F. de; TAVARES, M. E. da N.; TEIXEIRA, P. J. B. Avaliação da Capacidade Resistente e da Aderência de Elementos da Marquise do Estádio do Maracanã. Engenharia Estudo e Pesquisa, Rio de Janeiro, v. 13, n. 2, p. 3–9, 2014.

SRINIVASAN, S.; KANE, R. D. Experimental Simulation of Multiphase CO2/H2S Systems. CORROSION 99, [s. l.], 1999.

STERN, M.; WEISERT, E. D. Experimental observations on the relation between polarization resistance and corrosion rate. Proc. Am. Soc. Test. Mater, [s. l.], v. 59, p. 1280, 1959.

TEYMOURI, F. et al. Passive film alteration of reinforcing steel through [MoO42−]/[RCOO−] interfacial co-interaction for enhanced corrosion resistance in chloride contaminated concrete pore solution. [S. l.: s. n.], 2022.

TIAN, Y. et al. Cr-modified low alloy steel reinforcement embedded in mortar for two years: Corrosion result of marine field test. Cement and Concrete Composites, [s. l.], v. 97, p. 190–201, 2019.

TIAN, H. et al. Triazolyl-acylhydrazone derivatives as novel inhibitors for copper corrosion in chloride solutions. Corrosion Science, [s. l.], v. 100, p. 341–352, 2015. Disponível em: http://dx.doi.org/10.1016/j.corsci.2015.08.022.

TRAN, V. T. et al. Magnetic Layer-by-Layer Assembly: From Linear Plasmonic Polymers to Oligomers. ACS Applied Materials and Interfaces, [s. l.], v. 12, n. 14, p. 16584–16591, 2020.

URRA MEDINA, E.; BARRÍA PAILAQUILÉN, R. M. Systematic Reviews and Meta-analysis: Understanding the Best Evidence in Primary Healthcare. Revista latino-americana de enfermagem, [s. l.], v. 18, n. 4, p. 824–831, 2010.

VELEVA, L. et al. Comparative cyclic voltammetry and surface analysis of passive films grown on stainless steel 316 in concrete pore model solutions. Journal of Electroanalytical Chemistry, [s. l.], v. 537, p. 85–93, 2002.

VITÓRIO, J. A. P. Fundamentos da patologia das estruturas nas perícias de engenharia. Instituto Pernambucano de Avaliações e Perícias de Engenharia, [s. l.], p. 58, 2003.

WAGNER, C.; TRAUD, W. Zeitschrift fur Elektrochemie und angewandte physikalische Chemie. Elektrochem, [s. l.], v. 44, p. 391–454, 1938.

XU, P. et al. Corrosion inhibition efficiency of compound nitrite with D-sodium gluconate on carbon steel in simulated concrete pore solution. Construction and Building Materials, [s. l.], v. 288, p. 123101, 2021. Disponível em: https://doi.org/10.1016/j.conbuildmat.2021.123101.

XU, P. et al. Influence of sulfate salt type on passive film of steel in simulated concrete pore solution. Construction and Building Materials, [s. l.], v. 223, p. 352–359, 2019.

XU, J.; TAN, Q.; MEI, Y. Corrosion protection of steel by Mg-Al layered double hydroxides in simulated concrete pore solution: Effect of SO42-. Corrosion Science, [s. l.], v. 163, n. September 2019, 2020.

YANG, R.-J. et al. Effect of sodium d-gluconate-based inhibitor in preventing corrosion of reinforcing steel in simulated concrete pore solutions. Acta Physico-Chimica Sinica, [s. l.], v. 28, n. 8, p. 1923–1928, 2012.

YANG, H. et al. Preparation of corrosion inhibitor loaded zeolites and corrosion resistance of carbon steel in simulated concrete pore solution. Construction and Building Materials, [s. l.], v. 225, p. 90–98, 2019. Disponível em: https://doi.org/10.1016/j.conbuildmat.2019.07.141.

YAO, N. et al. Synergistic effect of red mud and fly ash on passivation and corrosion resistance of 304 stainless steel in alkaline concrete pore solutions. Cement and Concrete Composites, [s. l.], v. 132, 2022.

ISSN: 1696-8352

ZHAI, M. et al. Layered double hydroxides (LDHs) modified cement-based materials: A systematic review. Nanotechnology Reviews, [s. l.], v. 11, n. 1, p. 2857–2874, 2022.

ZHAO, Yazhou et al. Corrosion inhibition efficiency of triethanolammonium dodecylbenzene sulfonate on Q235 carbon steel in simulated concrete pore solution. Corrosion Science, [s. l.], v. 158, n. June, p. 108097, 2019. Disponível em: https://doi.org/10.1016/j.corsci.2019.108097.

ZHAO, Y et al. Corrosion inhibition efficiency of triethanolammonium dodecylbenzene sulfonate on Q235 carbon steel in simulated concrete pore solution. Corrosion Science, [s. l.], v. 158, 2019.

ZHENG, H. et al. Influence of calcium ion in concrete pore solution on the passivation of galvanized steel bars. Cement and Concrete Research, [s. l.], v. 108, n. October 2017, p. 46–58, 2018. Disponível em: https://doi.org/10.1016/j.cemconres.2018.03.001.

ZHI, F. et al. Inhibition effect and mechanism of polyacrylamide for steel corrosion in simulated concrete pore solution. Construction and Building Materials, [s. l.], v. 259, p. 120425, 2020. Disponível em: https://doi.org/10.1016/j.conbuildmat.2020.120425.

ZIMER, A. M. Estudo da corrosão do aço ao carbono em meio de sulfeto. 2009. 241 f. - UFSCar, São Carlos, 2009.